Mixed Langmuir Monolayers of Gramicidin A and Ethyl Palmitate: Pressure−Area Isotherms and Brewster Angle Microscopy

ARTICLE *in* THE JOURNAL OF PHYSICAL CHEMISTRY B · AUGUST 2002

Impact Factor: 3.3 · DOI: 10.1021/jp0140926

4 AUTHORS, INCLUDING:

Patrycja Dynarowicz-Latka
Jagiellonian University
177 PUBLICATIONS **1,951** CITATIONS

SEE PROFILE

Mixed Langmuir Monolayers of Gramicidin A and Ethyl Palmitate: Pressure−Area Isotherms and Brewster Angle Microscopy

N. Vila-Romeu,*,† M. Nieto-Suárez,† P. Dynarowicz-Łątka,§ and I. Prieto†

Department of Physical Chemistry, Faculty of Sciences, University of Vigo; Campus As Lagoas, s/n 32004 Ourense, Spain, and Department of General Chemistry, Faculty of Chemistry, Jagiellonian University, Ingarderna 3, 30-060 Kraków, Poland

Received: November 8, 2001; In Final Form: April 24, 2002

Isotherms of surface pressure, π, against mean molecular area, A, were obtained for monolayers of gramicidin A (GA), ethyl palmitate (EP), and mixtures of the two spread at the air−water interface of aqueous solutions of $CaCl_2$ at 15, 20, and 25 °C. Plots of A and of monolayer collapse pressure (π_c) against mole fraction of GA (X_{GA}) both suggest miscibility between GA and EP in monolayers at the working temperatures. The morphology of GA, EP, and GA/EP monolayers on aqueous NaCl and $CaCl_2$ solutions at these temperatures was studied by Brewster angle microscopy. The two-dimensional GA/EP solution containing numerous small microdomains of condensed phase was visualized at any surface pressure.

Introduction

Gramicidin A (GA), a polypeptide antibiotic produced by *Brevibacillus brevis*,[1] is one of the best-characterized and most intensively studied channel-forming peptides (even though it is not clear that channel formation is really its principal natural functional role). The primary structure of the monomer is a linear chain of 15 amino acids with hydrophobic side groups, D amino acids alternating with L amino acids. In most environments, however, GA exists in one or more of a number of tubular dimeric forms: left- or right-handed double helices formed by coiling parallel or antiparallel two-stranded β-sheets and left- or right-handed single helices formed by head-to-head hydrogen bonding between the amino terminals of two similarly helical monomers. In all of these tubular configurations, the peptide backbone forms the inside of the tube and the hydrophobic side groups the outside; which forms predominate depends in ill-understood ways on the solvent, the temperature, the nature and concentrations of any ions present in solution, and the nature of any lipid layer or bilayer in which the GA molecules may be embedded (in particular, its thickness, curvature, and charge properties). When inserted in a suitable lipid layer or bilayer, at least two types of GA dimer act as one-way channels for the passage of monovalent cations but are blocked by divalent cations.[2−14]

At the air−water interface, GA appears to exist as antiparallel double-stranded β-helices and forms stable Langmuir films.[14] Its properties in this state, and its effects on any other components of the film, can therefore be studied by monolayer techniques.[15] Such films are of interest not only as models of biological membranes[16] but also for the development of synthetic selective ion-channelling membranes for use in chemosensors and other devices. For the latter purpose, it is necessary that, in the presence of the ions to be transported, GA is miscible with the membrane matrix in which its molecules are to be embedded and that its ability to transport those ions is not reduced by interaction with this matrix, by interaction with other ions that may be present in solution, or by moderate changes in temperature.

In a previous study,[18] we found that in the presence of Na^+ ions at 20 °C GA is indeed miscible in monolayers with ethyl palmitate (EP), a lipid with an uncharged, hydrophobic head that (i) reduces the likelihood of undesirable interactions with GA or with the ions to be transported and (ii) facilitates the transfer of films formed on water to solid supports. In fact, GA/EP mixing was quasi-ideal; in particular, the presence of EP did not alter the values of 14−19 mN m^{-1} at which plots of surface pressure, π, against mean molecular area, A, showed a plateau attributed to reorientation of the β-helical GA molecules from horizontal (parallel to the interface) to vertical (perpendicular to the interface).[17,18]

Here, we report the results of a similar $\pi-A$ study of GA/EP monolayers in the presence of Ca^{2+} ions at temperatures of 15, 20, and 25 °C and of Brewster angle microscopy (BAM) of GA/EP monolayers on aqueous solutions of Na^+ or Ca^{2+} ions. Because the phase transitions induced by compression of the film bring about morphological alterations that in turn cause changes in surface refractive index, this latter technique offers the possibility of direct visual detection of such transitions.[19,20]

In this work, we have extended our investigations into the influence of divalent (Ca^{2+}) ions on the properties of gramicidin A/ethyl palmitate monolayers and the effect of the temperature on the behavior of this system. Furthermore, to obtain further insight into the structure of such a system, we have employed a Brewster angle microscope (BAM) for direct display of pure and mixed monolayer morphologies.[19,20] The variation of molecular densities upon film compression, causing changes of the phase state of monolayers, allows the visualization of the morphological features and miscibility over a wide region of surface pressures.

Material and Methods

Gramicidin A (>90% pure, <5% H_2O) was purchased from Fluka and stored at 4 °C. Ethyl palmitate (98% pure) was supplied by Sigma Chemical Co. and stored at a temperature

* To whom correspondence should be addressed. Phone: +34988387095. Fax: +34988387001. E-mail: nvromeu@uvigo.es.
† University of Vigo.
§ Jagiellonian University.

10.1021/jp0140926 CCC: $22.00
Published on Web 08/30/2002

below 0 °C. Both compounds were used as received. GA/EP spreading solutions were prepared by mixing appropriate volumes of stock solutions of GA and EP, both dissolved in Merck spectroscopy grade chloroform.

Monolayer compression isotherms were obtained using a KSV-3000 LB system (total trough area 855 cm^2) placed on an antivibration table, and surface pressure was measured to a precision of ± 0.05 mN m^{-1} with a platinum Wilhelmy plate. Each Langmuir monolayer was prepared by depositing a sample of a spreading solution on an aqueous subphase consisting of a solution of NaCl or $CaCl_2$ (both 99.5% pure, from Merck) in ultrapure water (resistivity 18.2 MΩ cm) obtained using coupled Nanopure (Infinity) and Milli-Q water purification systems; Na^+ concentration was always 1×10^{-2} M and Ca^{2+} concentration 3×10^{-3} M (total solution ionic strength 0.01 M). Once spread, monolayers were left to equilibrate for 30 min before the start of compression. Monolayer compression was performed at a barrier speed of 0.64×10^{-2} nm^2 $molecule^{-1}$ min^{-1}. The desired working temperature (15, 20, or 25 °C) was controlled thermostatically to within 0.1 °C by a circulating water system.

Brewster angle microscopy was performed with a lateral resolution of 2 μm using a BAM 2 Plus microscope (NFT, Germany). p-Polarized light with a wavelength of 690 nm from a 30 mW laser was reflected at the Brewster angle (approximately 53.1°) off monolayers that had been left to equilibrate for at least 10 min at constant area. The images so obtained were digitized and processed to optimize image quality; those shown herein correspond to 228×170 μm^2 segments of the monolayer, the larger dimension being from side to side of the page.

Results and Discussion

***π*−*A* Isotherms.** As on pure water,[21] on $CaCl_2$ solutions, EP monolayers had strongly temperature-dependent $\pi-A$ isotherms; increasing the temperature caused the transition from the expanded to the condensed state to shift from a surface pressure of about 4 to 10 mN m^{-1} and the opposite trend in the monolayer collapse pressure, which fell from about 34 to 25 mN m^{-1} (Figure 1a−c, curve 1). The $\pi-A$ isotherms of GA monolayers on $CaCl_2$ solutions (Figure 1a−c, curve 2) all showed two regions of different compressibility separated by a plateau that sloped gently up between mean molecular areas of 235 and 155 $Å^2$ and that is attributed, as in previous studies,[14,18,22,23] to the reorientation of β-helical GA molecules from horizontal to vertical. Temperature had relatively little effect on the GA isotherms, the most significant being a fall in the surface pressure at which the horizontal-to-vertical transition began (π_t) from 19 mN m^{-1} at 15 and 20 °C to 14 mN m^{-1} at 25 °C. For fixed low surface pressure (<14 mN m^{-1}), raising temperature above 20 °C also expanded the monolayer.

The $\pi-A$ isotherms of the mixed GA/EP monolayers (Figure 1a−c, curves 3−5) generally resemble those of GA, though with smaller mean molecular areas for a given surface pressure. None show any signs of a phase transition or collapse at surface pressures at which EP monolayers undergo these processes (which is interpreted as reflecting the miscibility of GA and EP), but all, regardless of temperature or GA content, exhibit a plateau with a π_t of about 19 mN m^{-1}, close to that of the pure GA monolayers at temperatures below 25 °C.

At all temperatures, the surface pressure at which monolayer collapse began, π_c, depended nonlinearly on X_{GA}, the mole fraction of GA in the monolayer (Figure 2a−c). According to the two-dimensional phase rule,[24] this variation with X_{GA} is also a clear indication of the mutual miscibility of the components in the monolayer.

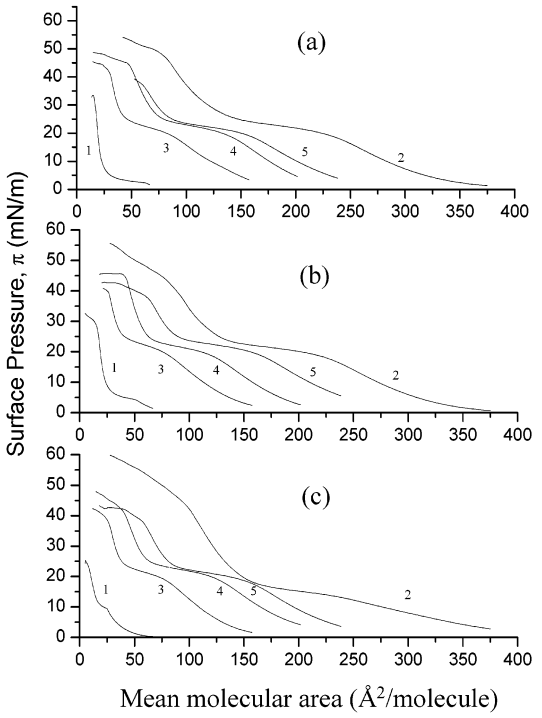

Figure 1. Surface pressure−area ($\pi-A$) isotherms of monolayers of EP (curve 1), GA (curve 2), and GA/EP mixtures with $X_{GA} = 0.33$ (curve 3), $X_{GA} = 0.5$ (curve 4), and $X_{GA} = 0.66$ (curve 5) spread on $CaCl_2$ solution ($I = 0.01$ M) at (a) 15, (b) 20, and (c) 25 °C.

Further evidence of miscibility comes from the X_{GA} dependence of mean molecular area, A. For binary monolayers formed of immiscible components or of miscible components 1 and 2 that either do not interact or have 1−2 interactions identical to the 1−1 and 2−2 interactions in films of the pure components (ideal mixing), A is additive:[25]

$$A = X_1A_1 + X_2A_2 \qquad (1)$$

where A_i is the mean molecular area of pure component i films at the relevant surface pressure and X_i is the mole fraction of component i in the mixed film. Figure 3a−c shows clear deviation from this linear behavior by GA/EP monolayers, although the extent of the deviation depends on both temperature and surface pressure. The dotted lines illustrate the additive relationship. Positive deviations correspond to repulsive molecular interactions between components,[26−28] while negative ones are characteristic of contraction of the two-component film due to attractive forces.[29−31] At 15 °C (Figure 3a), positive deviation from linearity at surface pressures below π_t (<19 mN m^{-1}) indicates nonideal mixing of the film components, the greatest interaction occurring at $X_{GA} = 0.5$, whereas at surface pressures of 25 or 30 mN m^{-1} (higher than the plateau), there appears to be little deviation from ideal mixing behavior. At 20 °C the $A-X_{GA}$ plots are nearly linear at all surface pressures (Figure 3b); but this is hardly likely to be due to immiscibility, because raising the temperature a little more makes them nonlinear again in a certain range of surface pressures (Figure 3c). Specifically, at 25 °C the $A-X_{GA}$ plots show positive deviation from linearity at surface pressures of 10−20 mN m^{-1} (i.e., between the π_t of EP and that of the mixed films), and again peak interaction is observed for $X_{GA} = 0.5$. At surface pressures that are outside this range, whether lower (Figure 3c) or higher (results not shown), the $A-X_{GA}$ plots are almost linear at this temperature.

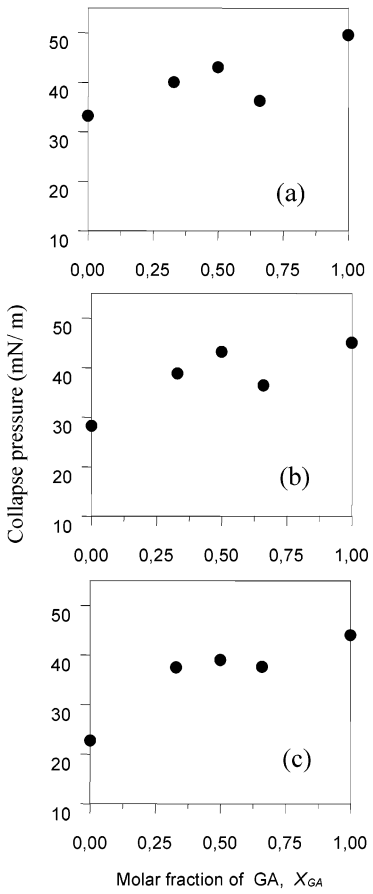

Figure 2. Influence of mole fraction of GA (X_{GA}) on the collapse pressures, π_c, of GA/EP monolayers spread on $CaCl_2$ solution (I = 0.01 M) at (a) 15, (b) 20, and (c) 25 °C.

The above results may be interpreted as follows. At 15 °C and surface pressures between the π_t of EP and that of the mixed films (4 and 19 mN m^{-1}, respectively; see Figure 1a), the hydrophobic tails of the lipid molecules rise essentially perpendicular to the interface, while the tubular GA molecules remain horizontal. The latter therefore considerably increase the average distance between EP molecules and cannot themselves interact strongly with their tails; this makes the hydrophobic attractions experienced by the EP molecules significantly weaker than those in pure EP films, which in turn results in the contribution of EP to mean molecular area being larger than that for ideal mixing. By contrast, at surface pressures above the π_t of GA, the axes of the GA molecules, like the EP tails, are oriented perpendicular to the interface; this allows hydrophobic GA−EP interactions of similar intensity to those present in pure EP or pure GA films at these surface pressures so results in quasi-ideal $A-X_{GA}$ behavior.

At 25 °C, both EP and GA molecules may be assumed to lie essentially parallel to the air−water interface at surface pressures below 10 mN m^{-1}, the value of π_t for EP at this temperature. Intermolecular interactions are therefore likely to be similar to those experienced in the pure films, and mixing behavior is accordingly quasi-ideal. At surface pressures between the π_t of EP and that of GA (10−20 mN m^{-1}), EP tails must be vertical and GA helices horizontal, resulting in positive deviation from linear $A-X_{GA}$ behavior for the same reasons as in the previous paragraph. At surface pressures greater than 20 mN m^{-1}, both molecules are vertical and the mixing behavior is once more quasi-ideal.

Brewster Angle Microscopy. BAM images were obtained at mean molecular area values typical of the expanded, transition, and condensed states of pure and mixed monolayers on Na^+ and Ca^{2+} solutions at 15, 20, and 25 °C.

(i) Pure Monolayers. At surface pressures in the transition region, pure EP monolayers spread on pure water at 15 and 20 °C show rounded, light-shaded areas of fluid-condensed film surrounded by a dark matrix of the fluid-expanded phase, while at 25 °C dendritic domain structures begin to appear.[21,32,33] In the presence of Na^+ or Ca^{2+} ions, the fluid-condensed domains are smaller and their borders exhibit numerous bright spots that may indicate nucleation sites for the transition from the expanded to the condensed state.[33]

Pure GA monolayers on Na^+ solutions at 15 °C (Figure 4a−d) or 20 °C (results not shown) have a completely homogeneous appearance at all of the mean molecular areas examined except the smallest, at which the onset of collapse is reflected by the appearance of linear fractures in the film (Figure 4d). At lower surface pressures, no coexistence of expanded and condensed domains was observed, nor was any difference between images taken at mean molecular areas corresponding to expanded and condensed states (Figure 4a−c). By contrast, on Ca^{2+} solutions at 15 °C (Figures 4e−h), the compression of GA films first brought about the appearance of small, bright, apparently randomly distributed microdomains that may indicate nucleation sites for the expanded-to-condensed transition (Figure 4f). Then, at pressures corresponding to the condensed state, compression

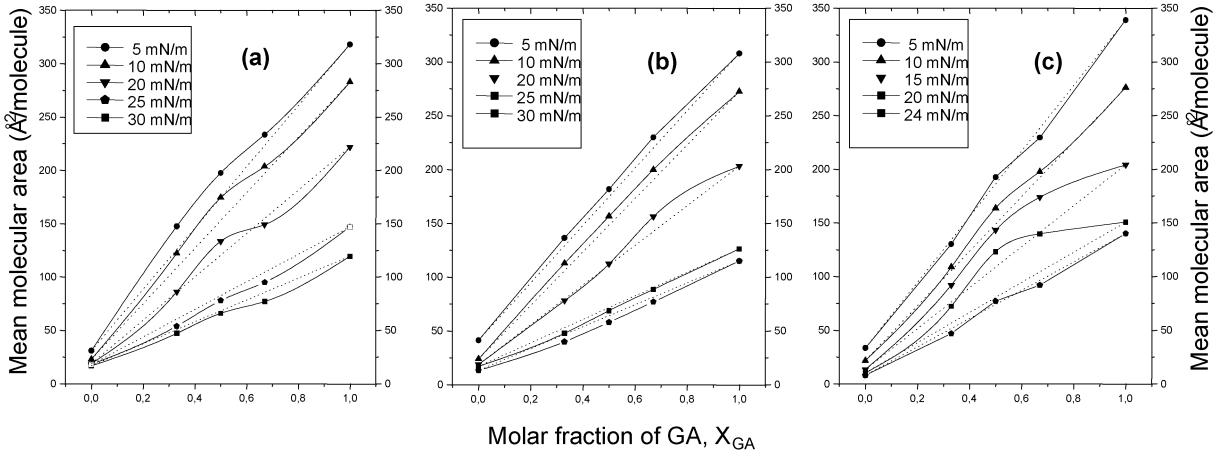

Figure 3. Influence of mole fraction of GA (X_{GA}) on the mean molecular areas, A, of GA/EP monolayers spread on $CaCl_2$ solution (I = 0.01 M) at (a) 15, (b) 20,and (c) 25 °C at various surface pressures.

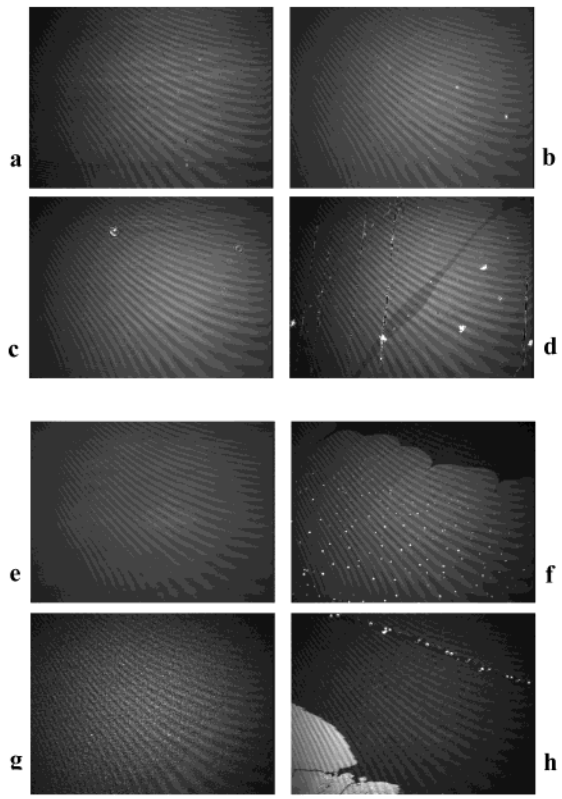

Figure 4. BAM images of pure GA monolayers with mean molecular areas, *A*, of (a,e) 340, (b,f) 130, (c,g) 110, and (d,h) 50 Å^2 on aqueous subphases containing Na^+ ions (a−d) or Ca^{2+} ions (e−h) at 15 °C.

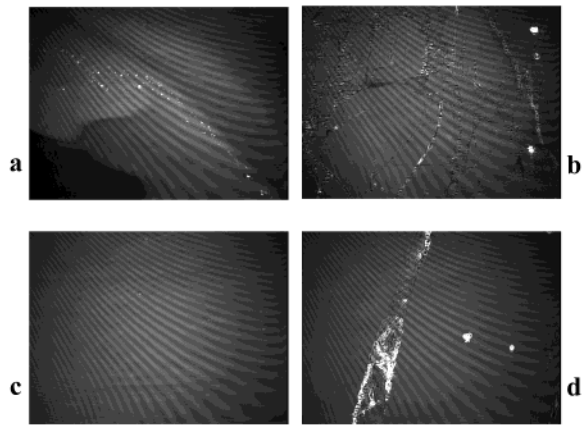

Figure 5. BAM images of pure GA monolayers with mean molecular areas, *A*, of (a,c) 140 and (b,d) 60 Å^2 on aqueous subphases containing Na^+ ions (a,b) or Ca^{2+} ions (c,d) at 25 °C.

caused the whole film to adopt a granular appearance (Figure 4g), possibly as the result of close juxtaposition of large numbers of small, condensed domains comprising densely packed, vertically oriented GA molecules. Upon final collapse, the film shows both linear series of what appear to be collapse nucleation sites (Figure 4h, top right) and dense, light-shaded collapsed areas (Figure 4h, bottom left).

At 25 °C, greater thermal agitation results in collapsing pure GA monolayers with an area of 60 Å/molecule spread on Na^+ solutions showing more fracture lines than films of 50 Å/molecule at 15 °C (Figures 4d and 5b). On Ca^{2+} solutions, the structures developed by collapsing pure GA films of 60 Å/molecule differ from those observed on 50 Å/molecule films at 15 °C, consisting of clusters of small dense (bright) areas arranged along fracture lines.

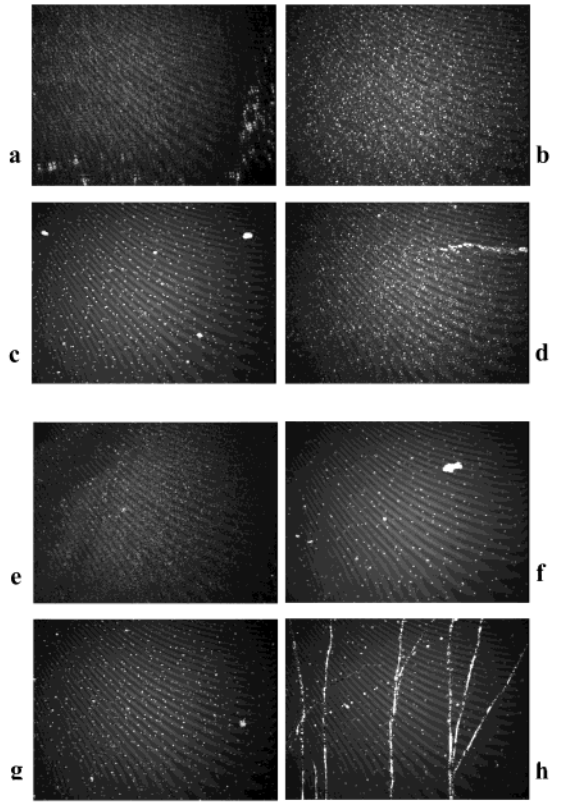

Figure 6. BAM images of mixed GA/EP monolayers ($X_{GA} = 0.5$) with mean molecular areas, *A*, of (a,e) 270, (b,f) 150, (c,g) 100, and (d,h) 50 Å^2 on aqueous subphases containing Na^+ ions (a−d) or Ca^{2+} ions (e−h) at 25 °C.

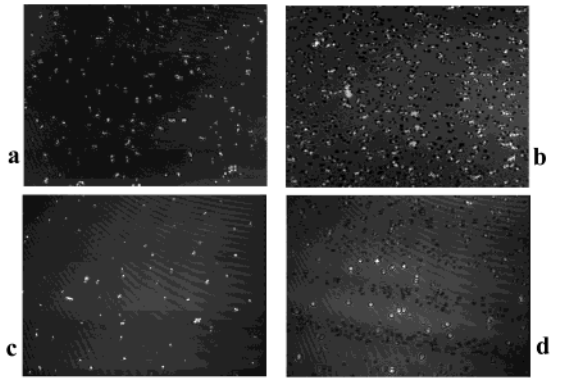

Figure 7. BAM images of mixed GA/EP monolayers ($X_{GA} = 0.5$) on aqueous subphases containing Na^+ ions (a, $A = 100$ Å^2; b, $A = 40$ Å^2) or Ca^{2+} ions (c, $A = 100$ Å^2; d, $A = 150$ Å^2) at 25 °C.

(ii) Mixed Monolayers. In states ranging from fully expanded to near collapse, equimolar GA/EP films at 25 °C showed large numbers of bright microdomains on both Na^+ and Ca^{2+} solutions (Figure 6). The number density of these microdomains is lowest at $X_{GA} = 0.1$ (Figure 7), increases with X_{GA} up to $X_{GA} = 0.5$ (Figure 6), and falls progressively at higher X_{GA}; the BAM images of mixed films with $X_{GA} \geq 0.8$ (on Ca^{2+} solutions) or ≥ 0.9 (Na^+) (not shown) are very similar to those of pure GA monolayers (Figure 5). The large refractive indices of the microdomains are attributable to dense packing of molecules, suggesting that the predominant fluid expanded phase of the film (dark area) coexists with random populations of aggregates in a condensed state (bright microdomains). The presence of these condensed states shows that addition of EP to GA monolayers does not have the fluidizing effect that has

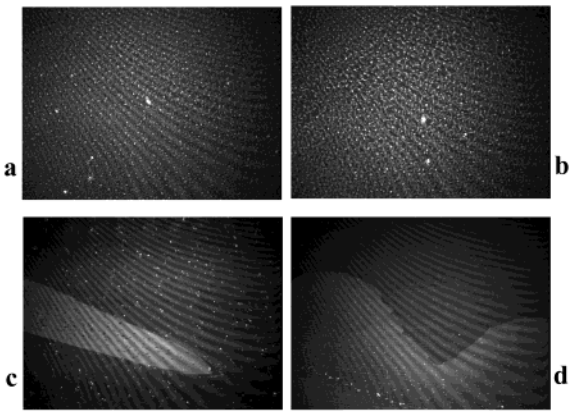

Figure 8. BAM images of mixed GA/EP monolayers ($X_{GA} = 0.5$) with mean molecular areas, *A*, of (a,c) 200 and (b,d) 100 Å^2 on aqueous subphases containing Na^+ ions (a,b) or Ca^{2+} ions (c,d) at 20 °C.

been reported for addition of cholesterol or fatty acids or both to other highly dense homogeneous monolayers.[34,35] Comparison of the 1:1 mixed monolayers formed on Na^+ and Ca^{2+} solutions at mean molecular areas of 150 Å (Figure 6b,f) shows that during compression of the expanded phase, at surface pressures of about 15 mN m^{-1}, the number density of microdomains is lower in the presence of divalent ions than in the presence of monovalent ions; such results would suggest that the formation of aggregates of GA/EP would be favored in the presence of Na^+ ions. This would be in keeping with the thermodynamic data; $A-X_{GA}$ curves for films spread on Ca^{2+} solutions at surface pressure of 15 mN m^{-1} exhibit positive deviation from ideal behavior (Figure 3c).

Temperature had only a quantitative effect with respect to the density of microdomains on the appearance of 1:1 mixed film BAM images in the presence of Na^+ (Figures 6a−d and 8a,b; images recorded at 15 °C are similar). In the presence of Ca^{2+}, however, 1:1 films had the appearance described in the previous paragraph at both 25 °C (Figure 6e−h) and 15 °C (not shown), but at 20 °C, macroscopic areas of differing reflectivities suggest the separation of areas with different GA orientation in both the transition region (Figure 8d) and the expanded phase (Figure 8c).

Conclusions

The behavior of the collapse pressures and $A-X_{GA}$ curves obtained from $\pi-A$ isotherms recorded at 15 and 25 °C in the presence of Ca^{2+} ions is compatible with GA and EP being miscible and interacting in monolayers spread at the air−water interface, mean molecular area deviating positively from ideal mixing behavior (greatest deviation occurring at $X_{GA} = 0.5$) at surface pressures at which EP molecules may be assumed to be oriented perpendicular to the interface and GA molecules parallel to it; the relevant surface pressure range is about 4−19 mN m^{-1} at 15 °C and 10−20 mN m^{-1} at 25 °C. At 20 °C, the area of mixed GA/EP monolayers is additive with respect to the mole fractions of the components.

BAM images suggest that at 15 or 20 °C the surface-condensed state of pure GA monolayers spread on Ca^{2+} solutions consists largely of closely juxtaposed small condensed domains comprising densely packed, vertically oriented molecules. The morphologies of mixed monolayers support the conclusion that GA and EP are miscible and interact in monolayers spread at the air−water interface. Such morphologies of mixed GA/EP monolayers exhibit a dependence on temperature and the nature of any ions in the aqueous subphase.

Acknowledgment. This work was supported by the University of Vigo and by Xunta de Galicia under Project No. 64102K105.

References and Notes

(1) Sarges, R.; Witkop, B. *J. Am. Chem. Soc.* **1965**, *87*, 2011−2015.
(2) Killian, J. A.; Urry, D. W. *Biochemistry* **1988**, *27*, 7295−7301.
(3) Cox, K. J.; Ho, C.; Lombardi, J. V.; Stubbs, C. D. *Biochemistry* **1992**, *31*, 1112−1118.
(4) Franks, N. P.; Lieb, W. R. *Nature* **1982**, *300*, 487−493.
(5) Franks, N. P.; Lieb, W. R. *Nature* **1988**, *333*, 662−664.
(6) Franks, N. P.; Lieb, W. R. *Nature* **1986**, *319*, 77−78.
(7) Henry, B. M.; Elliot, J. R.; Haydon, D. A. *Proc. R. Soc. London* **1985**, *B224*, 389−397.
(8) Haydon, D. A.; Henry B. M.; Lewinson, S. R.; Requena, J. *Nature* **1977**, *268*, 356−358.
(9) Haydon, D. A. *Ann. N. Y. Acad. Sci.* **1975**, *284*, 2−16.
(10) Hladky, S. B.; Haydon, D. A. *Curr. Top. Membr. Transp.* **1984**, *21*, 327−372.
(11) Salom, D.; Abad, C.; Braco, L. *Biochemistry* **1992**, *31*, 8072−8079.
(12) Scarlata, S. F. *Biochemistry* **1991**, *30*, 9853−9859.
(13) Nelson, A. *Langmuir* **1997**, *13*, 5644−5651.
(14) Ducharme, D.; Vaknin, D.; Paudler, M.; Salesse, C.; Riegler, H.; Möhwald, H. *Thin Solid Films* **1996**, *90*, 284−285.
(15) Gaines, G. L., Jr. *Insoluble Monolayers at Liquid−Gas Interface*; Interscience: New York, 1966.
(16) Maget-Dana, R. *Biochim. Biophys. Acta* **1999**, *109*, 1462.
(17) Mita, T. *Bull. Chem. Soc. Jpn.* **1993**, *66*, 1490.
(18) Vila, N.; Puggelli, M.; Gabrielli, G. *Colloids Surf., A* **1996**, *119*, 95−104.
(19) Hönig, D.; Möbius, D. *Thin Solid Films* **1992**, *210/211*, 64−68.
(20) Möbius, D. *Curr. Opin. Colloid Interface Sci.* **1996**, *1*, 250−256.
(21) Weidemann, G.; Vollhardt, D. *Langmuir* **1997**, *13*, 1623−1628.
(22) Tournois, H.; Gieles, P.; Demel, R.; de Gier, J.; De Kruijff, B. *Biophys. J.* **1989**, *55*, 557−565.
(23) Davion-Van Mau, N.; Daumas, P.; Lelièvre, D.; Trudelle, Y.; Heitz, H. *Biophys. J.* **1987**, *51*, 843−851.
(24) Crisp, D. J. *Surface Chemistry*; Butterworth: London, 1949; Supplement to Research, pp 17, 23−35.
(25) Goodrich, F. C. *Proc. 2nd Int. Congr. Surf. Act.* **1957**, *1*, 33−36.
(26) Pagano, R. E.; Gershfeld, N. L. *J. Phys. Chem.* **1972**, *76*, 1238−1244.
(27) Alsina, M. A.; Mestres, C.; Valencia, G.; Garcia Anton, J. M.; Reig, F. *Colloids Surf.* **1988**, *34*, 151−159.
(28) Angelova, A. *Thin Solid Films* **1994**, *243*, 394−401.
(29) Gilardoni, A.; Margheri, E.; Gabrielli, G. *Colloids Surf.* **1992**, *68*, 235−241.
(30) Bonosi, F.; Margheri, E.; Gabrielli, G. *Colloids Surf.* **1992**, *65*, 287−294.
(31) Petrov, J. G.; Möbius, D.; Angelova, A. *Langmuir* **1992**, *8*, 201−211.
(32) Gutberlet, T.; Vollhardt, D. *J. Colloid Interface Sci.* **1995**, *173*, 429−438.
(33) Nieto-Suárez, M.; Vila-Romeu, N.; Dynarowicz-Łątka, P.; Prieto, I. *J. Colloid Interface Sci.*, submitted for publication.
(34) Slotte, J. P.; Mattjus, P. *Biochim. Biophys. Acta* **1995**, *1254*, 22−29.
(35) Subramaniam, S.; McConnell, H. M. *J. Phys. Chem.* **1987**, *91*, 1715−1718.